

Supporting Information

Modeling Metal Influence on the Gate Opening in ZIF-8 Materials

Jenny G. Vitillo^{a,b,} and Laura Gagliardi^c*

^aDepartment of Science and High Technology and INSTM, Università degli Studi dell'Insubria, Via Valleggio 9, I-22100 Como, Italy.

^bDepartment of Chemistry, Chemical Theory Center, and Supercomputing Institute, University of Minnesota, 207 Pleasant Street S.E., Minneapolis, Minnesota 55455, United States.

^cDepartment of Chemistry, Pritzker School of Molecular Engineering, James Franck Institute, University of Chicago, Chicago, IL 60637, United States.

*E-mail: jg.vitillo@gmail.com

Table of Contents

S1. Additional data on electronic band structure and density of states (DOS) of ZIF-8 materials	2
S2. Additional data on the CASSCF and CASPT2 calculations	7

S1. Additional data on electronic band structure and density of states (DOS) of ZIF-8 materials

The electronic band structure and the density of states of ZIF-8(Zn)-AP (part a), ZIF-8(Zn)-HP (b), ZIF-8(Mg)-AP (c), and ZIF-8(Fe)-IP (d) are compared in Figure S1.

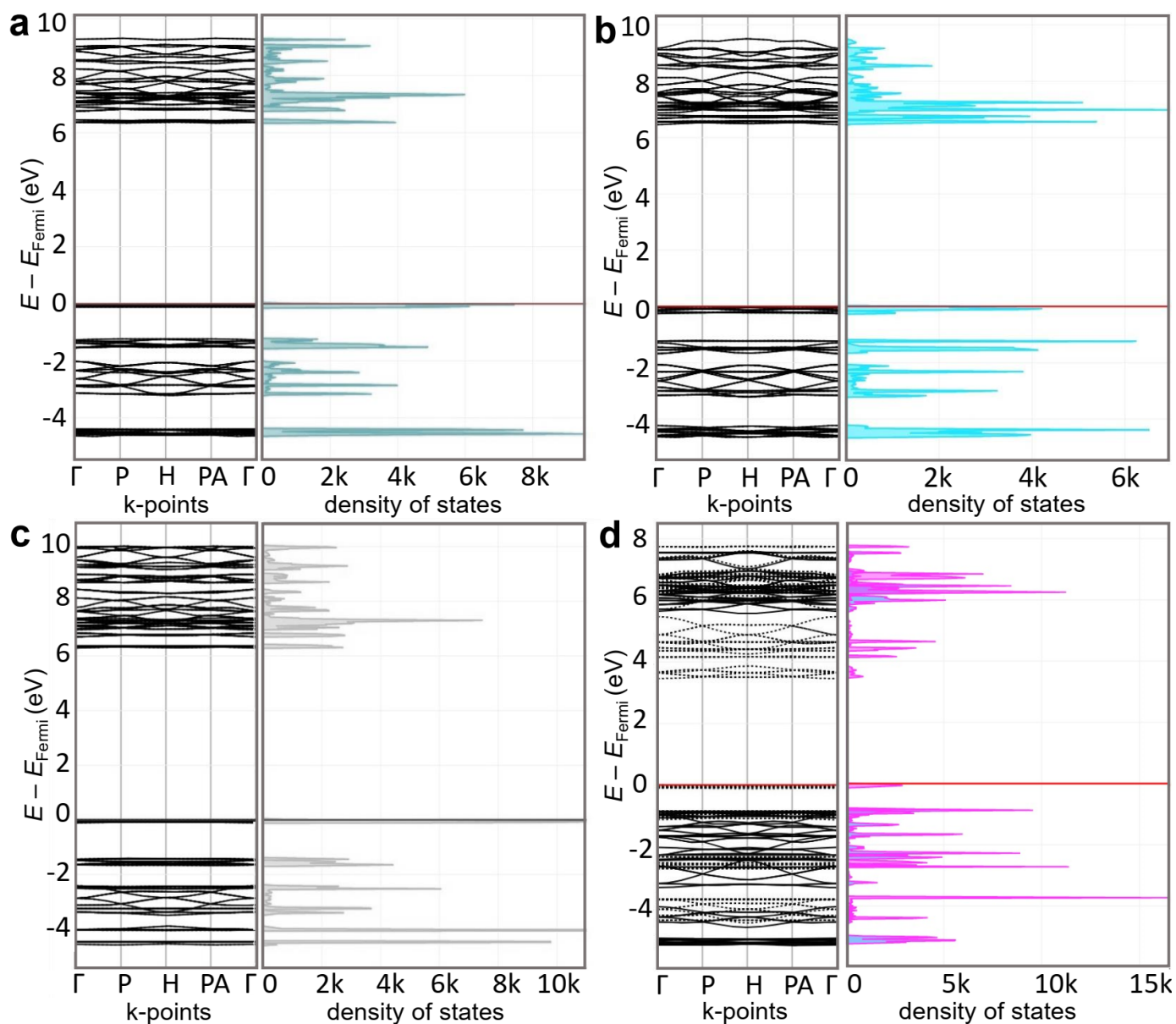


Figure S1. Electronic band structure and density of states (DOS) of (a) ZIF-8(Zn)-AP, (b) ZIF-8(Zn)-HP, (c) ZIF-8(Mg)-AP, and (d) ZIF-8(Fe)-IP ($2S+1 = 49$) obtained at the B3LYP-D*/TZVp level. In (d), blue and pink areas correspond to alpha and beta electrons, respectively.

The next plots show the total density of states (light blue) and its projected values for each atom of the asymmetric unit for ZIF-8(Zn)-AP (Figure S2), ZIF-8(Zn)-HP (Figure S3), ZIF-8(Mg)-AP (Figure S4), and ZIF-8(Fe)-IP (Figure S5). It is evident that while for Zn and Mg the band gap is mainly associated to imidazolate orbitals, for Fe the band gap orbitals have a main contribution from the iron orbital.

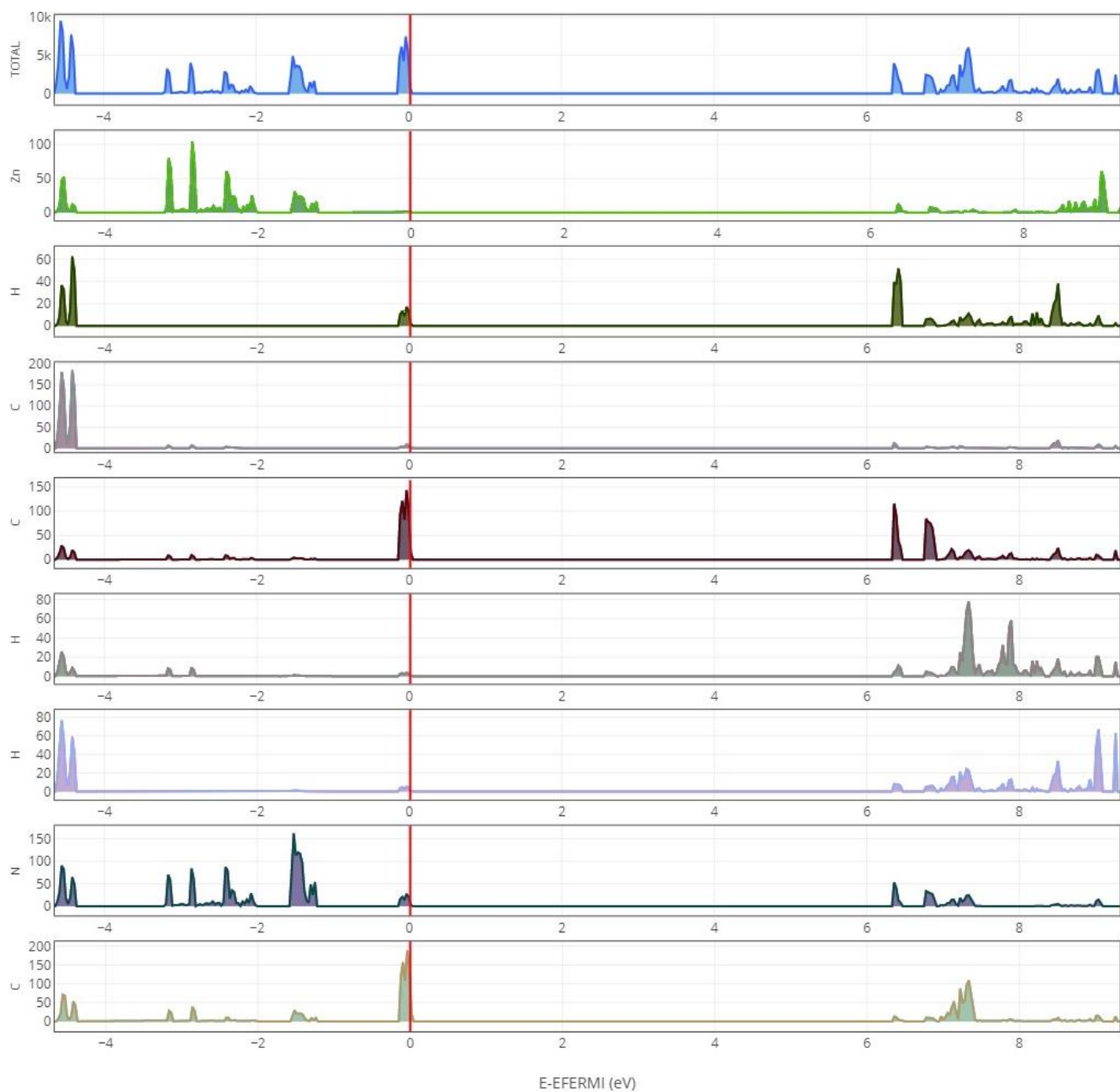


Figure S2. Projected density of states (DOS) of ZIF-8(Zn)-AP obtained at the B3LYP-D*/TZVp level.

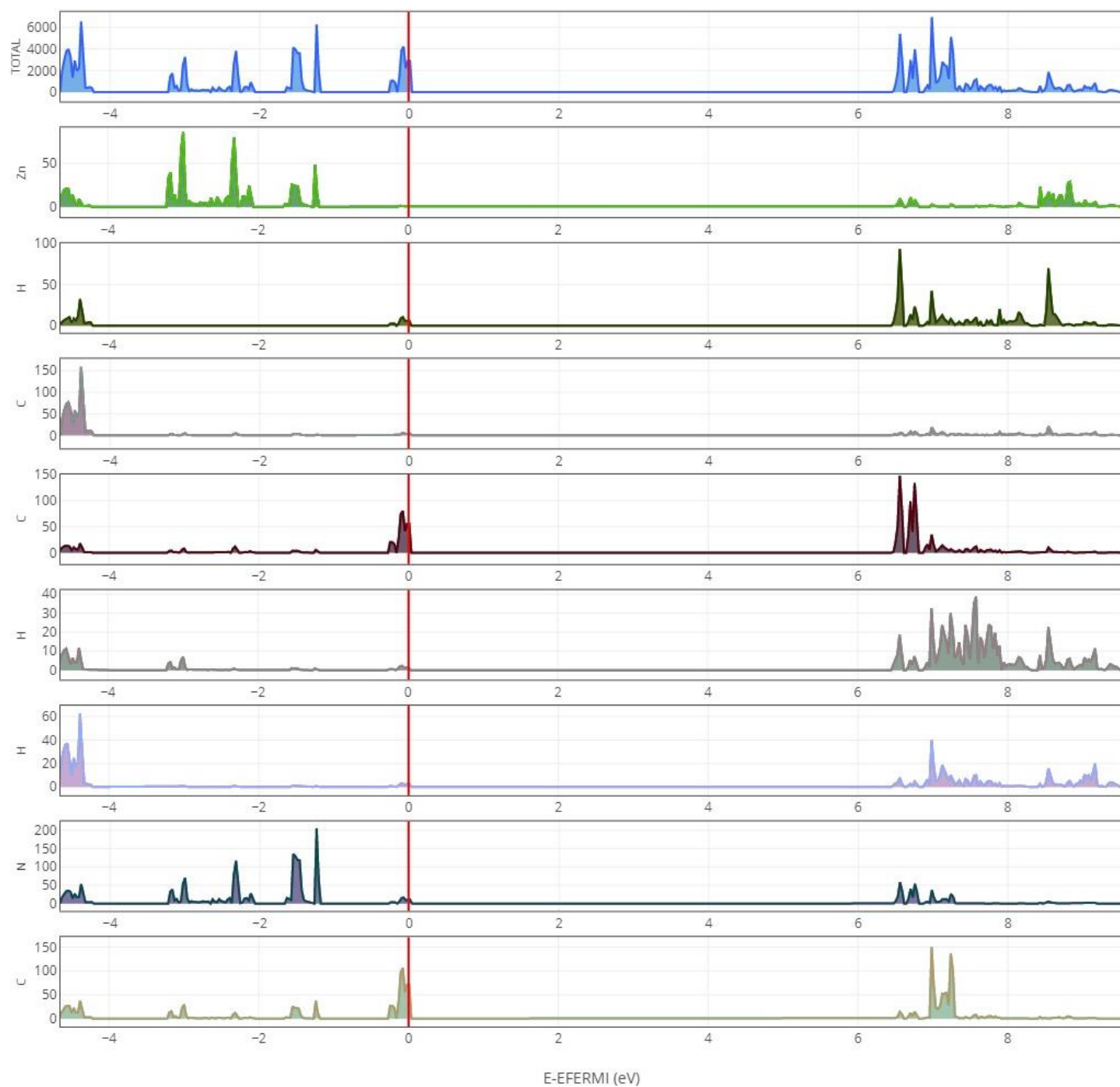


Figure S3. Projected density of states (DOS) of ZIF-8(Zn)-HP obtained at the B3LYP-D*/TZVp level.

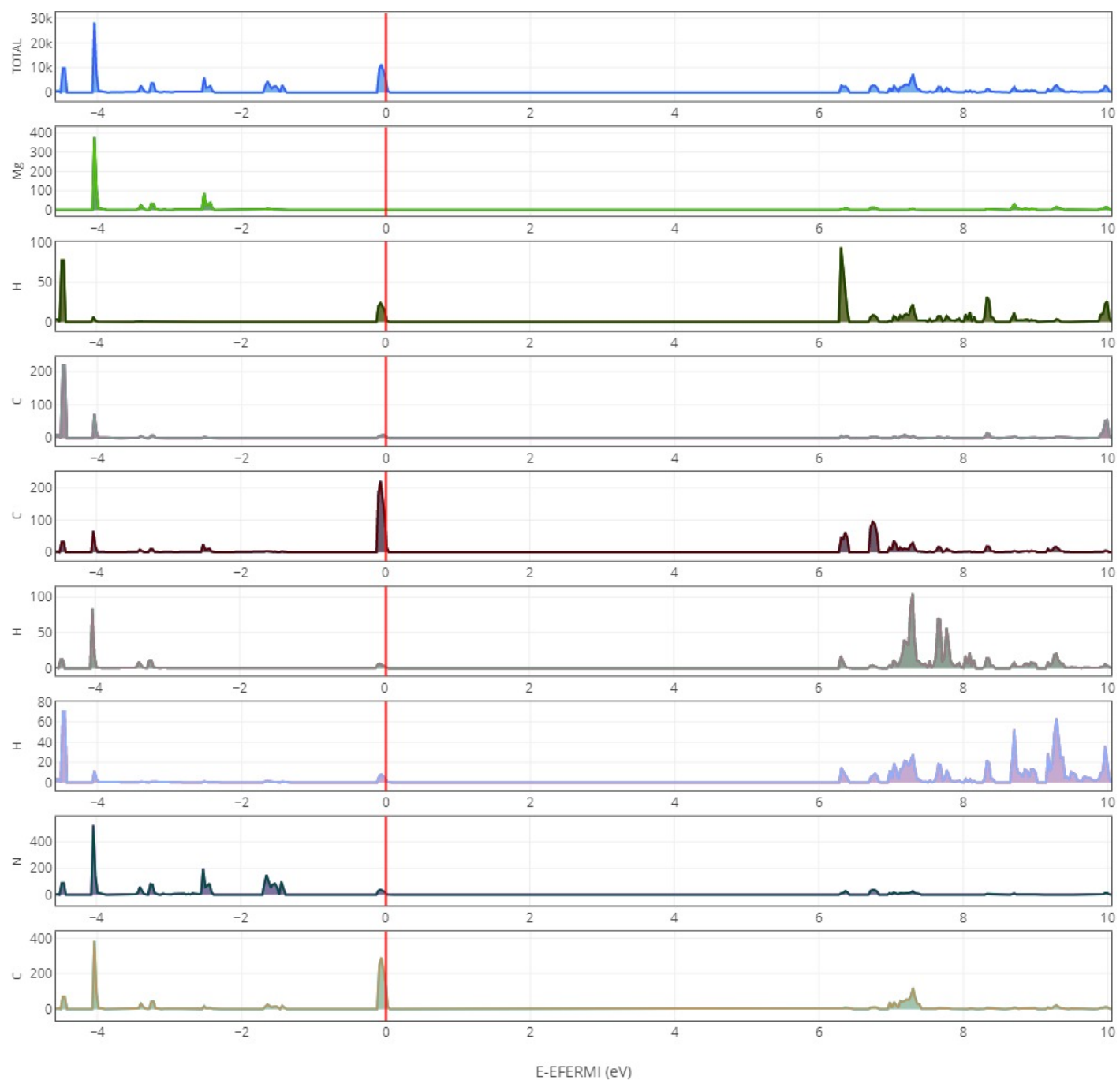


Figure S4. Projected density of states (DOS) of ZIF-8(Mg)-AP obtained at the B3LYP-D*/TZVp level.

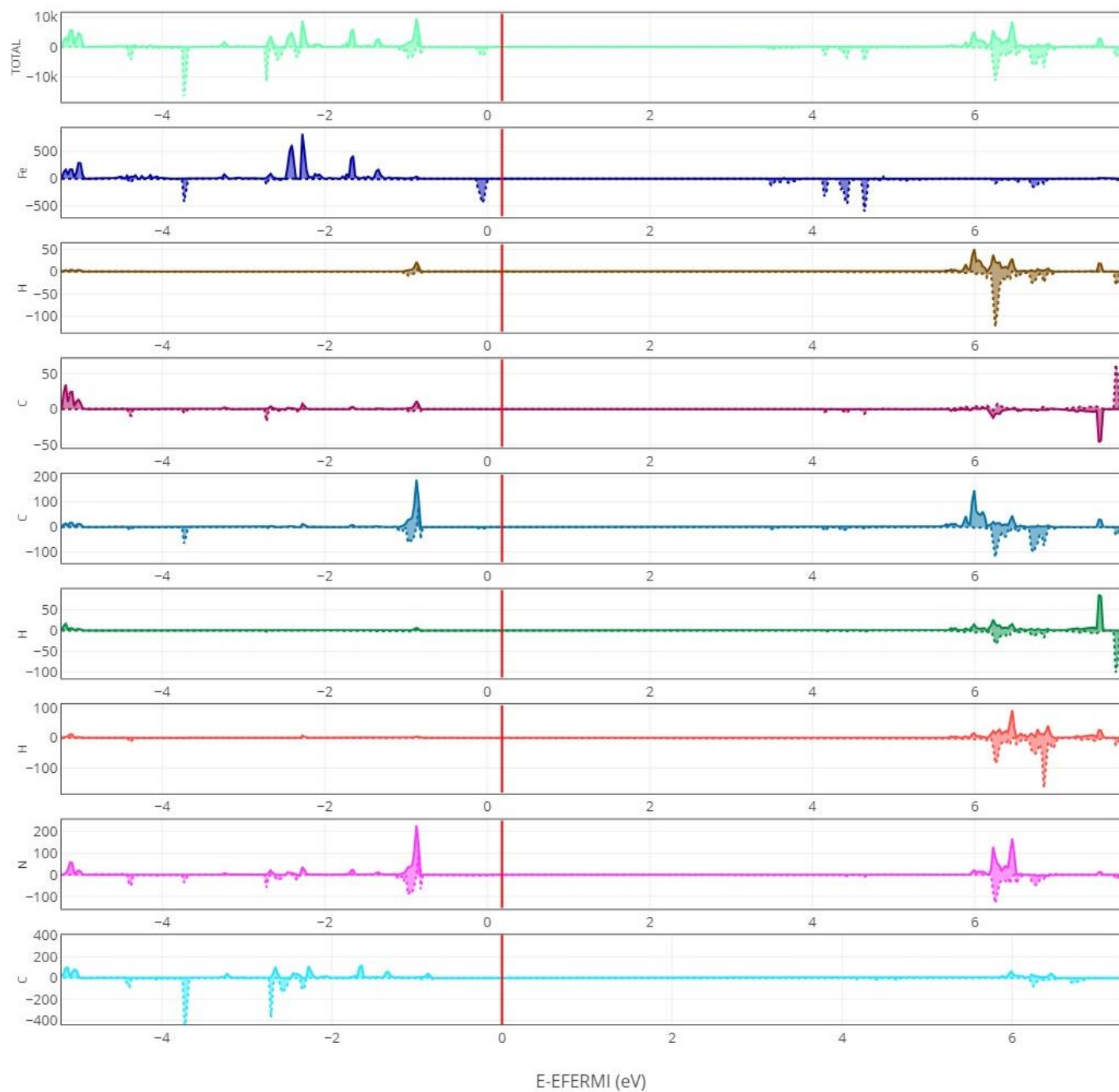


Figure S5. Projected density of states (DOS) of ZIF-8(Fe)-AP ($2S+1 = 49$) obtained at the B3LYP-D*/TZVp level. Positive and negative values correspond to alpha and beta electrons, respectively.

S2. Additional data on the CASSCF and CASPT2 calculations

Single points calculations were performed using multireference methods on Fe₁ and Fe₂ clusters (see Figure S6), carved from the B3LYP-D* optimized structure of ZIF-8(Fe)-IP ($2S + 1 = 49$).

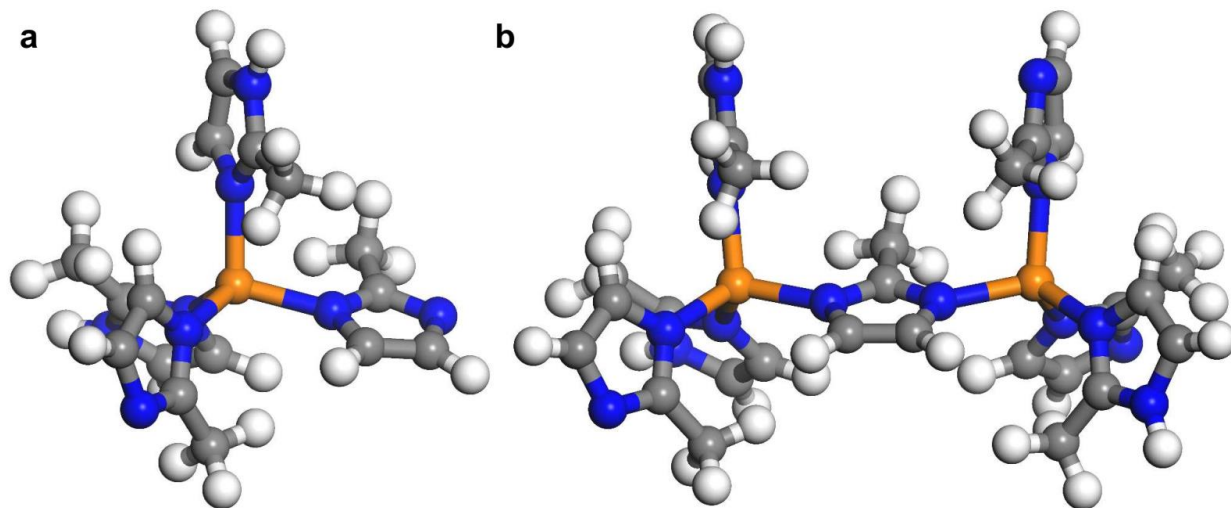


Figure S6. Mono-iron cluster Fe₁ and di-iron cluster Fe₂ carved from ZIF-8(Fe)-IP ($2S + 1 = 49$) structure and used for multireference wave function based calculations. Color code of the atoms: iron (orange), N (blue), C (grey), H (white).

In **Table S1**, the CASSCF and CASPT2 relative stability of the singlet, triplet, and pentet for the Fe₁ cluster is reported for increasing dimension of the active space. The relative energy of the spin states at the CASPT2 level has a very small dependence on the active space dimension. The pentet is the most stable spin state, followed by the triplet and the singlet. The orbitals and their occupancy for the pentet are showed in **Table S2**: it is evident as both the occupied and unoccupied orbitals composing the (4,10) active space are mainly contributed from 3d and 3d' atomic orbitals of iron (see also **Table S3**). The results are invariant also on the basis set (compare **Table S1** and **Table S2**), validating the use of the smaller basis set for Fe₂, being the larger one not affordable.

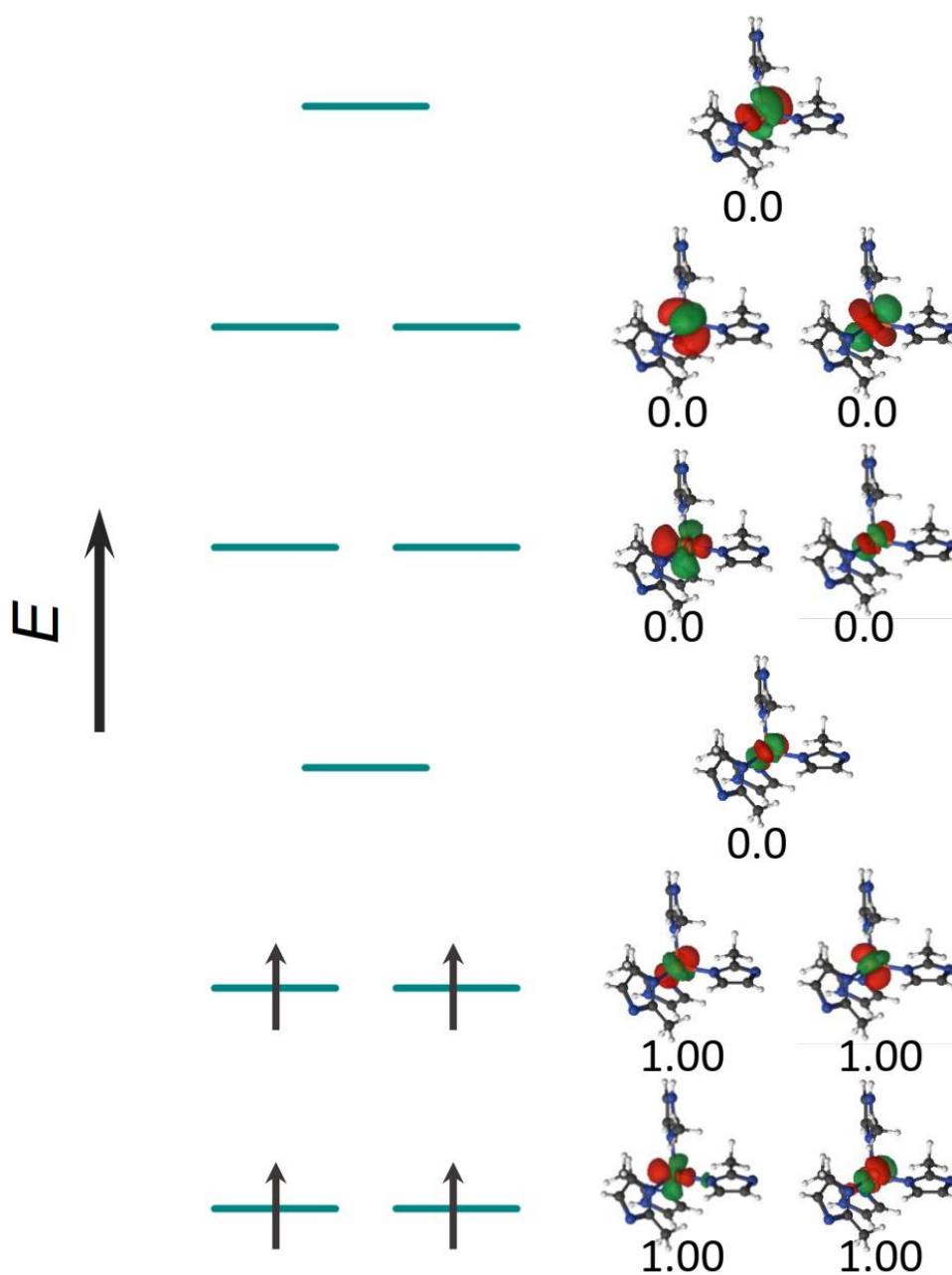


Figure S7. Qualitative molecular orbital diagram showing the natural orbitals for a mono-iron cluster Fe_1 for $S = 2$ obtained at the CASSCF(4,10) level using the largest basis set. Color code as in Figure 6.

Table S1. Relative energy stability obtained by single point calculations on the mono-iron cluster Fe₁ at the CASSCF and CASPT2 level of theory using (4,5) active spaces using two different basis set (small and large, see Computational Methods) for increasing spin multiplicities (2S + 1). All the values are in kJ mol⁻¹.

2S + 1	small basis set		large basis set	
	$\Delta E(\text{CASSCF})$	$\Delta E(\text{CASPT2})$	$\Delta E(\text{CASSCF})$	$\Delta E(\text{CASPT2})$
1	345.7	372.9	345.5	370.6
3	217.4	237.6	217.2	235.9
5	0.0	0.0	0.0	0.0

Table S2. Relative energy stability obtained by single point calculations on the mono-iron cluster Fe₁ at the CASSCF and CASPT2 level of theory using (4,10) active spaces using two different basis set (small and large, see Computational Methods) for increasing spin multiplicities (2S + 1). All the values are in kJ mol⁻¹.

2S + 1	small basis set		large basis set	
	$\Delta E(\text{CASSCF})$	$\Delta E(\text{CASPT2})$	$\Delta E(\text{CASSCF})$	$\Delta E(\text{CASPT2})$
1	313.9	370.6	314.5	371.8
3	203.3	234.1	203.2	234.5
5	0.0	0.0	0.0	0.0

Table S3. Relative energy stability obtained by single point calculations on the di-iron cluster Fe₂ at the CASSCF and CASPT2 level of theory using (8,10) and (8,20) active spaces for increasing spin multiplicities (2S + 1). All the values are in kJ mol⁻¹.

2S + 1	(8,10)		(8,20)	
	$\Delta E(\text{CASSCF})$	$\Delta E(\text{CASPT2})$	$\Delta E(\text{CASSCF})$	$\Delta E(\text{CASPT2})$
1	0.0	0.0	0.0	0.4
3	0.0	1.1	0.0	1.5
5	0.0	1.7	0.0	1.9
7	0.0	2.1	0.0	1.8
9	0.1	1.7	0.1	0.0

Figure S8. Output of the CASSCF calculation for the mono-iron cluster Fe₁ using a (4,10) active space for $S = 2$ and the larger basis set reporting the occupancy and the coefficients for each natural orbital calculation. MOLCAS labeling of the spherical harmonics is: $3d_{2+} = 3d_{x^2-y^2}$, $3d_{1+} = 3dxz$, $3d_0 = 3d_{z^2}$, $3d_{1-} = 3dyz$, $3d_{2-} = 3dxy$.

```

99  0.0000  0.9964
22 FE1 3d2- ( 0.1080) 25 FE1 3d1- ( 0.2817) 28 FE1 3d0 (-0.3341) 31 FE1 3d1+ ( 0.1979)
34 FE1 3d2+ ( 0.8649)
100 0.0000 0.9972
22 FE1 3d2- ( 0.2810) 25 FE1 3d1- (-0.7508) 28 FE1 3d0 (-0.4980) 31 FE1 3d1+ ( 0.3161)
61 N2 2s ( 0.1098)
101 0.0000 0.9970
22 FE1 3d2- (-0.4507) 25 FE1 3d1- (-0.1975) 28 FE1 3d0 (-0.4320) 31 FE1 3d1+ (-0.7362)
34 FE1 3d2+ ( 0.1238) 61 N2 2s (-0.1035) 91 N3 2s ( 0.1283) 100 N3 2pz (-0.1001)

102 0.0000 0.9965
22 FE1 3d2- ( 0.8294) 25 FE1 3d1- ( 0.1583) 31 FE1 3d1+ (-0.5104) 241 N8 2s (-0.1270)
271 N9 2s ( 0.1156)
103 0.0000 0.0031
29 FE1 4d0 (-0.4251) 30 FE1 5d0 ( 0.2830) 32 FE1 4d1+ ( 0.1873) 33 FE1 5d1+ (-0.1241)
35 FE1 4d2+ ( 0.6788) 36 FE1 5d2+ (-0.4452)
104 0.0000 0.0028
23 FE1 4d2- ( 0.2963) 24 FE1 5d2- (-0.1989) 26 FE1 4d1- (-0.6693) 27 FE1 5d1- ( 0.3975)
29 FE1 4d0 (-0.3499) 30 FE1 5d0 ( 0.2246) 35 FE1 4d2+ (-0.2535) 36 FE1 5d2+ ( 0.1644)
61 N2 2s ( 0.1738) 241 N8 2s (-0.2021) 497 C24 2s ( 0.1204)
105 0.0000 0.0005
37 FE1 4f3- ( 0.7708) 39 FE1 4f2- ( 0.2964) 41 FE1 4f1- (-0.1535) 45 FE1 4f1+ (-0.2274)
47 FE1 4f2+ (-0.4619) 49 FE1 4f3+ ( 0.1770)
106 0.0000 0.0030
14 FE1 4py ( 0.1389) 23 FE1 4d2- ( 0.6133) 24 FE1 5d2- (-0.4332) 26 FE1 4d1- ( 0.2398)
27 FE1 5d1- (-0.1521) 32 FE1 4d1+ (-0.4711) 33 FE1 5d1+ ( 0.3274) 241 N8 2s (-0.1777)
271 N9 2s ( 0.2191)
107 0.0000 0.0005
4 FE1 4s (-0.1714) 5 FE1 5s (-0.1229) 37 FE1 4f3- ( 0.1767) 39 FE1 4f2- (-0.4630)
41 FE1 4f1- (-0.1830) 43 FE1 4f0 ( 0.1174) 45 FE1 4f1+ ( 0.1541) 47 FE1 4f2+ (-0.3040)
49 FE1 4f3+ (-0.7693)
108 0.0000 0.0030
19 FE1 4pz (-0.1519) 23 FE1 4d2- ( 0.4609) 24 FE1 5d2- (-0.3011) 26 FE1 4d1- ( 0.1543)
29 FE1 4d0 ( 0.2559) 30 FE1 5d0 (-0.1756) 32 FE1 4d1+ ( 0.6212) 33 FE1 5d1+ (-0.4244)
61 N2 2s ( 0.1811) 91 N3 2s (-0.2151) 441 C20 2s ( 0.1008)

```

Figure S9. Output of the CASSCF calculation for the di-iron cluster Fe_2 using a (8,20) active space for $S = 0$ reporting the occupancy and the coefficients for each natural orbital calculation. MOLCAS labeling of the spherical harmonics is: $3d_{+2} = 3d_{x^2-y^2}$, $3d_{+1} = 3dxz$, $3d_0 = 3d_{z^2}$, $3d_{-1} = 3dyz$, $3d_{-2} = 3dxy$.

175	0.0000 81 FE2 232 N11	0.9969 3d2- 2s	(0.1014) (0.1011)	84 FE2 246 N12	3d1- 2s	(-0.4709) (-0.1146)	90 FE2 250 N12	3d1+ 2py	(0.3446) (0.1188)	93 FE2	3d2+	(-0.7905)
176	0.0000 81 FE2	0.9968 3d2- 2s	(0.8581)	87 FE2	3d0	(0.4926)						
177	0.0000 22 FE1	0.9960 3d2- 2s	(-0.8611)	25 FE1	3d1-	(0.1062)	28 FE1	3d0	(0.4703)	31 FE1	3d1+	(0.1070)
178	0.0000 22 FE1	0.9968 3d2- 2s	(0.3480)	25 FE1	3d1-	(0.6326)	28 FE1	3d0	(0.5743)	31 FE1	3d1+	(-0.3578)
179	0.0000 84 FE2 218 N10	0.9969 3d1- 2s	(0.6627) (-0.1150)	90 FE2 224 N10	3d1+ 2pz	(-0.4389) (-0.1041)	93 FE2	3d2+	(-0.5947)	204 N9	2s	(0.1027)
180	0.0000 25 FE1 288 N15	0.9964 3d1- 2s	(-0.4543) (0.1131)	28 FE1 290 N15	3d0 2px	(0.1655) (-0.1161)	31 FE1 302 N16	3d1+ 2s	(-0.4676) (-0.1020)	34 FE1	3d2+	(-0.7310)
181	0.0000 81 FE2	0.9972 3d2- 2s	(-0.3414)	84 FE2	3d1-	(0.3605)	87 FE2	3d0	(0.5698)	90 FE2	3d1+	(0.6480)
182	0.0000 22 FE1 34 FE1	0.9963 3d2- 3d2+	(0.1284) (-0.6537)	25 FE1 148 N5	3d1- 2s	(0.3831) (-0.1050)	28 FE1 162 N6	3d0 2s	(-0.1147) (0.1056)	31 FE1 168 N6	3d1+ 2pz	(0.6195) (-0.1067)
183	0.0000 23 FE1 82 FE2 88 FE2	0.0032 4d2- 4d2- 4d0	(-0.7137) (-0.1711) (-0.1611)	23 FE1 83 FE2	5d2- 5d2-	(0.3836) (0.1002)	29 FE1 85 FE2	4d0 4d1-	(0.3851) (-0.1974)	30 FE1 86 FE2	5d0 5d1-	(-0.2114) (0.1032)
184	0.0000 26 FE1 33 FE1 91 FE2 306 N16	0.0030 4d1- 5d1+ 4d1+ 2py	(-0.2718) (0.1488) (-0.1005) (0.1272)	27 FE1 35 FE1 288 N15	5d1- 4d2+ 2s	(0.1573) (-0.7822) (0.1537)	29 FE1 36 FE1 290 N15	4d0 5d2+ 2px	(0.1685) (0.4266) (-0.1563)	32 FE1 85 FE2 302 N16	4d1+ 4d1- 2s	(-0.2781) (0.1172) (-0.1468)
185	0.0000 37 FE1 47 FE1	0.0007 4f3- 4f2+	(-0.4154) (0.1820)	41 FE1 49 FE1	4f1- 4f3+	(-0.2688) (-0.7773)	43 FE1 50 FE1	4f0 5f3+	(-0.2974) (0.1096)	45 FE1	4f1+	(0.1117)
186	0.0000 37 FE1 45 FE1	0.0005 4f3- 4f1+	(0.3194) (0.4771)	39 FE1 47 FE1	4f2- 4f2+	(0.1603) (-0.6849)	41 FE1 49 FE1	4f1- 4f3+	(0.2391) (-0.2803)	43 FE1	4f0	(-0.1317)
187	0.0000 37 FE1 43 FE1	0.0006 4f3- 4f0	(0.2394) (-0.4798)	39 FE1 45 FE1	4f2- 4f1+	(0.7468) (-0.1127)	40 FE1 47 FE1	5f2- 4f2+	(-0.1056) (0.1133)	41 FE1 49 FE1	4f1- 4f3+	(-0.2570) (0.2262)
188	0.0000 23 FE1 33 FE1 92 FE2 246 N12	0.0031 4d2- 5d1+ 5d1+ 2s	(0.1586) (0.1276) (-0.2311) (-0.1303)	26 FE1 85 FE2 94 FE2 250 N12	4d1- 4d1- 4d2+ 2py	(-0.2254) (-0.5815) (-0.4031) (0.1242)	27 FE1 86 FE2 95 FE2	5d1- 5d1- 5d2+	(0.1179) (0.3017) (0.2090)	32 FE1 91 FE2 232 N11	4d1+ 4d1+ 2s	(-0.2496) (0.4130) (0.1032)
189	0.0000 32 FE1 92 FE2 210 N9	0.0031 4d1+ 5d1+ 2pz	(-0.1310) (-0.1034) (0.1038)	85 FE2 94 FE2 218 N10	4d1- 4d2+ 2s	(-0.3216) (0.8075) (0.1253)	86 FE2 95 FE2 224 N10	5d1- 5d2+ 2pz	(0.1656) (-0.4345) (0.1164)	91 FE2 204 N9	4d1+ 2s	(0.2127) (-0.1323)
190	0.0000 26 FE1 33 FE1 86 FE2 162 N6	0.0030 4d1- 5d1+ 5d1- 2s	(-0.3544) (0.3277) (-0.1373) (-0.1455)	27 FE1 35 FE1 91 FE2 168 N6	5d1- 4d2+ 4d1+ 2pz	(0.1878) (0.4347) (-0.1482) (0.1270)	29 FE1 36 FE1 148 N5	4d0 5d2+ 2s	(0.1606) (-0.2429) (0.1353)	32 FE1 85 FE2 154 N5	4d1+ 4d1- 2pz	(-0.6213) (0.2661) (0.1057)
191	0.0000 37 FE1 45 FE1	0.0007 4f3- 4f1+	(0.6862) (-0.4281)	39 FE1 49 FE1	4f2- 4f3+	(-0.1981) (-0.3821)	41 FE1	4f1-	(-0.3595)	43 FE1	4f0	(0.1420)
192	0.0000 26 FE1 83 FE2 89 FE2 206 N9	0.0028 4d1- 5d2- 5d0 2px	(-0.2197) (-0.1370) (0.2428) (-0.1027)	27 FE1 85 FE2 91 FE2 232 N11	5d1- 4d1- 4d1+ 2s	(0.1097) (-0.3016) (-0.5811) (-0.1267)	29 FE1 86 FE2 92 FE2 234 N11	4d0 5d1- 5d1+ 2px	(-0.1950) (0.1327) (0.2916) (-0.1099)	82 FE2 88 FE2 204 N9	4d2- 4d0 2s	(0.2817) (-0.5050) (0.1383)
193	0.0000 23 FE1 83 FE2	0.0032 4d2- 5d2-	(-0.2277) (-0.3891)	24 FE1 88 FE2	5d2- 4d0	(0.1129) (0.4108)	29 FE1 89 FE2	4d0 5d0	(0.1008) (-0.2165)	82 FE2	4d2-	(0.7404)
194	0.0000 23 FE1 29 FE1 82 FE2 148 N5	0.0028 4d2- 4d0 4d2- 2s	(-0.3186) (-0.4840) (-0.1490) (0.1262)	24 FE1 30 FE1 85 FE2 152 N5	5d2- 5d0 4d1- 2py	(0.1565) (0.2401) (0.1517) (0.1026)	26 FE1 32 FE1 88 FE2 302 N16	4d1- 4d1+ 4d0 2s	(-0.5857) (0.2755) (0.1579) (-0.1283)	27 FE1 33 FE1 91 FE2 306 N16	5d1- 5d1+ 4d1+ 2py	(0.2998) (-0.1296) (0.1700) (0.1098)